JCTC Journal of Chemical Theory and Computation

Article

pubs.acs.org/JCTC

Performance of PNOF5 Natural Orbital Functional for Radical Formation Reactions: Hydrogen Atom Abstraction and C−C and O−O Homolytic Bond Cleavage in Selected Molecules

Xabier Lopez,*[,†] Fernando Ruipérez,[†] Mario Piris,[†,‡] Jon M. Matxain,[†] Eduard Matito,[§] and Jesus M. Ugalde[†]

[†]Kimika Fakultatea, Euskal Herriko Unibertsitatea (UPV/EHU), and Donostia International Physics Center (DIPC), P.K. 1072, 20080 Donostia, Euskadi, Spain

[‡]IKERBASQUE, Basque Foundation for Science, 48011 Bilbao, Spain

[§]Department of Chemistry and Institute of Computational Chemistry, University of Girona, 17071 Girona, Catalonia, Spain

Supporting Information

ABSTRACT: Radical formation through hydrogen abstraction and C−C and O−O homolytic bond cleavage from selected molecules is investigated by use of natural orbital functional theory in its PNOF5 natural orbital functional implementation, and the results are compared to high-level ab initio complete active space self-consistent field (CASSCF) and complete active space with second-order perturbation theory (CASPT2) methods and experimental data. It is observed that PNOF5 is able to treat the strong electron correlation effects along the homolysis of X−H (X = C, N, O) and X−X (X = C, O) bonds, leading, in general, to the correct trends in the corresponding bond strengths and a good description of the resultant electronic structure for these radicals. In general, PNOF5 bond energies are lower than the experimental ones, because of partial lack of dynamical electron correlation. However, the part of dynamical electron correlation recovered by PNOF5 allows it to give more accurate results than CASSCF methods with a minimum window required to treat near-degeneracy effects. In addition, inspection of the natural orbital occupancies with respect to the CASSCF ones shows an outstanding performance of PNOF5 in treating degenerate and quasidegenerate states, giving a correct description of diradicals and diradicaloids formed upon C−C cleavage in cyclopropane and derivatives.

INTRODUCTION

Formation of radicals from homolysis of a covalent bond is an important process in chemistry, and it has profound implications in a variety of chemical areas, such as combustion, polymerization and oxidation of molecules, with impact in environmental, industrial, biological[1] and organic chemistry.[2] In particular, formation of radicals by hydrogen atom abstraction from aliphatic chains is a fundamental step to explain oxidation of hydrocarbons[3] and apolar side chains of proteins.[4−6] As observed for instance in lipid peroxidation,[7] carbon-centered radicals in the presence of oxygen can in turn form peroxyl radicals (ROO$^{\bullet}$) or alkoxy radicals or can be recombined to form C−C covalent bonds. In these processes, a key step is the formation of one or more reactive oxygen species[8] (ROS). Particularly important among ROS is the $^{\bullet}$OH radical, a key species found in atmospheric chemistry and responsible for hydrogen abstraction from a variety of organic molecules,[9,10] Fenton chemistry,[11] and DNA damage.[12] Another important ROS is hydroxyperoxyl radical, $HO_2^{\bullet}$, a key combustion intermediate in the oxidation of fuels and an oxidizer of volatile organic compounds.[13]

Proper description of the hydrogen atom abstraction pathway in a variety of basic hydrides is a first but fundamental step for accurate characterization of the electronic structure of these important species.[14−16] However, this requires the appropriate treatment of strong correlation effects, unfortunately not without difficulty. In wave function methods, the use of a single determinant, such as in Hartree−Fock (HF), provides incorrect results and, therefore, the need for a multiconfigurational wave function, leading to computationally expensive methods. Other alternatives, such as density functional theory (DFT), show important limitations to treat strong electron correlation or near-degeneracy effects.[17]

Natural orbital functional theory[18] (NOFT) is being configured as an alternative formalism to both DFT and wave function methods, by describing the electronic structure in terms of natural orbitals and their occupation numbers. Various functionals have been developed in recent years,[19−26] and comprehensive reviews can be found in refs 27 and 28. Within the class of Piris natural orbital functionals,[29−33] those satisfying the known D, Q, and G necessary conditions for the N-representability of the second-order reduced density matrix (2-RDM) are best suited to describe strong correlation effects.[27] Thus, the so-called PNOF4[32] functional can describe properly dissociation curves of a variety of molecules and the ethylene torsion potential. In addition, this functional has also demonstrated outstanding performance in the treatment of small diradicals and diradicaloids.[32b] More recently, a new version of PNOF has been developed, PNOF5,[33] which behaves correctly for a variety of molecules in various chemical type of bonding and bond orders. Moreover, PNOF5 leads to integral numbers

Received: March 30, 2012
Published: July 5, 2012

of electrons on the dissociated fragments.[33b] This is a cumbersome problem of present density and density matrix functionals, even for the variational 2-RDM approach, under the D, Q, and G positivity necessary conditions, which leads to incorrect dissociation limits with a fractional number of electrons on the dissociated atoms for a number of diatomic molecules.[34,35] However, this is an important property to describe radicals formed upon homolysis of covalent bonds. Due to the outstanding ability of PNOF5 to deal with homolysis in a variety of small molecules,[33] leading to dissociated radicals with integral numbers of electrons, in the present paper we will analyze the performance of PNOF5 to treat hydrogen abstraction in a variety of fundamental hydrides (CH_4, NH_3 and H_2O), leading to the formation of radicals. In addition, we also analyze the hydrogen abstraction in C_2H_6 and H_2O_2 and compare it with the homolysis of C−C and O−O bonds, respectively. Finally, we also take as a case study the C−C cleavage in a series of cyclopropane derivatives, forming molecules with full and partial radical character. We compare our results with state-of-the-art complete active space self-consistent field (CASSCF) and complete active space with second-order perturbation theory (CASPT2) methods, showing that PNOF5 is able to treat the strong correlation effects found in radical formation through hydrogen abstraction and X−X bond homolysis (X = C, O).

METHODS

Geometries were optimized at coupled cluster singles−doubles (CCSD) (in the case of CH_4, NH_3 and H_2O molecules), M06-2X[36] (for C_2H_6 and H_2O_2 species), and CASSCF(4,4) [trimethylenemethane (TMM), oxyallyl (OXA), iminoallyl (IMA), cyclopropane and its derivatives] levels of theory with the correlation-consistent valence double-ζ or triple-ζ basis set (cc-pVDZ and cc-pVTZ) developed by Dunning.[37] At these geometries, single-point energies were evaluated by use of HF, CASSCF(N_e,N_{orb}) (i.e., N_e electrons in N_{orb} orbitals), CASPT2-(N_e,N_{orb}), and PNOF5 (see below) levels of theory with various basis sets: cc-pVDZ, aug-cc-pVDZ, and cc-pVTZ. The effect of the basis set was nonrelevant for the discussion of this paper, and for the sake of brevity, only the cc-pVTZ results are shown, with the rest of the data provided as Supporting Information. In addition, in the case of CH_4, NH_3, H_2O, C_2H_6, and H_2O_2, CASSCF and CASPT2 calculations were performed with different window sizes. In this paper, we focus on the CASSCF(2,2) and CASPT2(2,2) calculations; larger-size CASSCF and CASPT2 results are also provided as Supporting Information. Geometry optimizations were carried out by use of the Gaussian09 program package,[38] and for the CASSCF and CASPT2 single-point energies the MOLCAS 7.4 program[39] was used.

The PNOF5 calculations were performed with the PNOFID code.[40] Next, we summarize the essentials of the theory; details can be found elsewhere.[33] If a real set of natural orbitals is assumed, the PNOF5 energy for a singlet state of an N-electron system can be cast as

$$E^{\mathrm{PNOF5}} = \sum_{p=1}^{N} [n_p(2H_{pp} + J_{pp}) - \sqrt{n_{\tilde{p}} n_p} K_{p\tilde{p}}] + \sum_{p,q=1}^{N}{}'' n_q n_p (2J_{pq} - K_{pq}) \quad (1)$$

where p denotes the spatial natural orbital and n_p is its occupation number. H_{pp} is the pth matrix element of the kinetic energy and nuclear attraction terms, whereas $J_{pq} = \langle pq|pq \rangle$ and $K_{pq} = \langle pq|qp \rangle$ are the usual Coulomb and exchange integrals, respectively. The $\tilde{p}$ state defines the coupled natural orbital to the orbital p, namely, $\tilde{p} = N - p + 1$, with N being the number of particles in the system and all occupancies vanishing for $p > N$. It is worth noting that we look for the pairs of coupled orbitals $(p, \tilde{p})$ that yield the minimum energy for the functional of eq 1, but the actual paired p and $\tilde{p}$ orbitals are not constrained to remain fixed along the orbital optimization process. We have found that this pairing accounts for the essential orbital interactions for a reliable description of the static correlation effects and assures dissociation limits with integer number of electrons at the dissociated parts. The double prime in eq 1 indicates that both the $q = p$ term and the coupled one-particle state terms $p = \tilde{p}$ are omitted from the last summation. Additionally, the bounds on the necessary conditions for the N-representability of the 2-RDM and the sum rules of the 2-RDM that must be satisfied imply that the occupation of the $\tilde{p}$ level must coincide with that of the hole of its coupled state p, namely, $n_{\tilde{p}} = h_p$, where h_p denotes the hole $1 - n_p$ in the spatial orbital p. The solution in NOF theory is established by optimizing the energy functional with respect to the occupation numbers and to the natural orbitals separately, for which the recent successful implementation of an iterative diagonalization procedure has been employed.[41]

RESULTS

In this section, the obtained results are presented and discussed. First, hydrogen abstraction from CH_4, NH_3, and H_2O is studied, leading to $^{\bullet}CH_3$, $^{\bullet}NH_2$, and $^{\bullet}OH$ radicals. Then homolytic C−C and O−O bond cleavage is studied versus hydrogen abstraction in C_2H_6 and H_2O_2. Next, the bond dissociation energies are combined to yield reaction energies of a variety of hydrogen abstraction reactions induced by selected radicals. Finally, C−C homolytic bond cleavage in a group of cyclopropane derivatives is considered.

Hydrogen Abstraction. Here we discuss the cases for the hydrogen abstraction from basic hydrides, namely, the following reactions:

$$CH_4 \rightarrow {}^{\bullet}CH_3 + H^{\bullet}$$

$$NH_3 \rightarrow {}^{\bullet}NH_2 + H^{\bullet}$$

$$H_2O \rightarrow {}^{\bullet}OH + H^{\bullet}$$

In Figure 1, we depict the PNOF5 potential energy curves for these homolytic bond cleavages, and in Table 1, the resultant PNOF5, CASSCF, and CASPT2 dissociation energies (D_e) are listed. The three potential curves behave properly along the whole X−H reaction coordinate, as we stretch the X−H bond there is a gradual lowering of the occupation of the σ_{XH} bonding orbital and an increase in the occupation of the σ^*_{XH} antibonding orbital. At the asymptotic limit, all cases show occupations of 1.0/1.0 for these two orbitals, describing therefore a homolytic X−H bond cleavage, and therefore, the formation of two radicals, $^{\bullet}XH_{n-1} + H^{\bullet}$ from XH_n (X = C, N, O).

Regarding the values of the dissociation energies, PNOF5 obtains a similar dissociation energy for the C−H and N−H bonds, 98.9 and 97.9 kcal/mol, respectively, and a significantly larger one for O−H, 106.1 kcal/mol. Note that the N−H and C−H experimental bond strengths are also very close in energy,

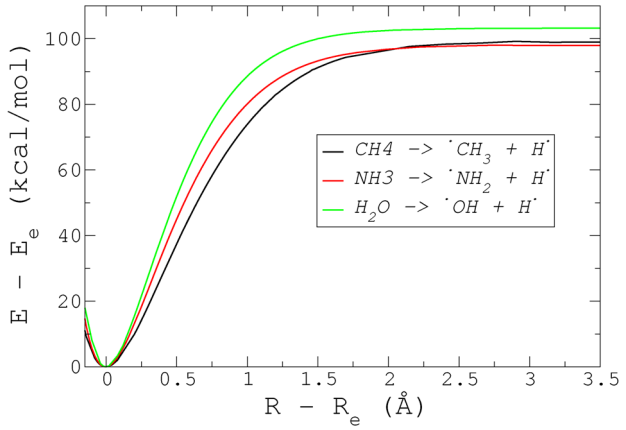

Figure 1. Hydrogen abstraction from XH_n hydrides (X = C, N, O). Data were obtained from PNOF5/cc-pVTZ single-point calculations at CCSD/cc-pVTZ partially optimized geometries with one of the X−H distances frozen.

but the N−H is slightly stronger by 3 kcal/mol while PNOF5 predicts C−H to be stronger by 1 kcal/mol. CASSCF(2,2) shows a serious failure in predicting the qualitative order of the X−H bond strength, with O−H and N−H bonds having weaker bonds than C−H. This wrong tendency is corrected upon introduction of dynamical electron correlation through CASPT2(2,2), and therefore, accurate calculation of dynamical electron correlation effects is crucial for predicting the correct trends of X−H bond strengths. Our results suggest that PNOF5 is able to take into account not only near-degeneracy effects along the dissociation process but also some of the relevant dynamical electron correlation to get the right qualitative trends. However, quantitative differences exist between PNOF5, CASSCF/CASPT2, and experimental data. CASSCF(2,2) results, which almost exclusively include strong correlation effects, underestimate X−H bond strengths by 16−33 kcal/mol. Inclusion of dynamical electron correlation effects significantly improves these results. CASPT2(2,2) underestimates experimental data by only 4 kcal/mol. PNOF5 results lie in between, underestimating experimental data by 15−20 kcal/mol. The PNOF5 underestimation of bond strengths has been previously noted,[33] and it is related to the mentioned partial lack of dynamical electron correlation, more important at the equilibrium structures than at the dissociation limit.

Homolytic Bond Cleavage versus Hydrogen Abstraction. In this section we study hydrogen abstraction from carbon and oxygen in ethane and hydrogen peroxide, respectively, in comparison with X−X homolytic bond cleavage (X = C, O) in the same molecule. Thus, the following reactions have been considered.:

Homolytic dissociations in ethane:

(a)

$$C_2H_6 \rightarrow {}^{\bullet}CH_3 + {}^{\bullet}CH_3$$

(b)

$$C_2H_6 \rightarrow {}^{\bullet}C_2H_5 + H^{\bullet}$$

Homolytic dissociations in hydrogen peroxide

(a)

$$H_2O_2 \rightarrow {}^{\bullet}OH + {}^{\bullet}OH$$

(b)

$$H_2O_2 \rightarrow HO_2^{\bullet} + H^{\bullet}$$

In Figure 2, the calculated PNOF5 dissociation curves are depicted, and the PNOF5, CASSCF(2,2) and CASPT2(2,2)

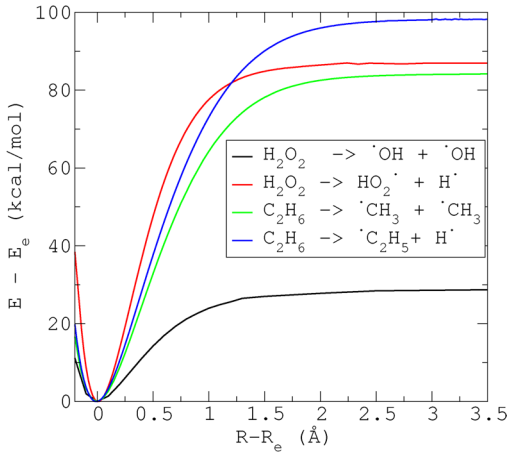

Figure 2. X−H and X−X homolytic bond cleavage in C_2H_6 and H_2O_2 molecules. Data were obtained from PNOF5/cc-pVDZ single-point calculations at M062X/cc-pVTZ partially optimized geometries with either X−X or one of the X−H distances frozen.

D_e values are collected in Table 2. Similarly to the dissociation curves of the X−H bonds in hydrides, these curves show the correct asymptotic behavior. According to the experimental results for these reactions and those of the previous section, one can see that (i) X−H bonds are stronger than X−X bonds, (ii) the O−O bond is significantly weaker than the C−C bond, and (iii) the O−H bond in peroxide is much weaker than the O−H bond in water, which is weaker in turn than the

Table 1. Formation of Radicals from X−H Bond Dissociation in Methane, Ammonia, and Water[a,b]

	D_e (kcal/mol)		
	$CH_4 \rightarrow {}^{\bullet}CH_3 + H^{\bullet}$	$NH_3 \rightarrow {}^{\bullet}NH_2 + H^{\bullet}$	$H_2O \rightarrow {}^{\bullet}OH + H^{\bullet}$
PNOF5	98.9	97.9	106.1
CASSCF(2,2)	98.0	93.3	92.9
CASPT2(2,2)	109.6	111.5	122.8
exptl	113.0	115.9	126.0

[a]Dissociation energies were calculated from single-point energies at CCSD/cc-pVTZ optimized geometries. Calculation of the energy at the dissociation limit was done at an X−H distance of 5 Å. [b]ZPVEs were added to the experimental dissociation energies.[42] ZPVE values were taken from the Computational Chemistry Comparison and Benchmark DataBase[43] and correspond to CCSD(T)/cc-pVTZ values.

dx.doi.org/10.1021/ct300414t | J. Chem. Theory Comput. 2012, 8, 2646−2652

Table 2. Formation of Radicals from Ethane and Hydrogen Peroxide upon X−H and X−X Homolysis[a,b]

	D_e (kcal/mol)			
	$C_2H_6 \rightarrow$		$H_2O_2 \rightarrow$	
	$^{\bullet}CH_3 + {}^{\bullet}CH_3$	$^{\bullet}C_2H_5 + H^{\bullet}$	$^{\bullet}OH + {}^{\bullet}OH$	$HO_2^{\bullet} + H^{\bullet}$
PNOF5	83.1	98.9	32.6	86.6
CASSCF(2,2)	74.2	89.2	19.4	81.3
CASPT2(2,2)	96.6	106.0	53.7	91.0
exptl	96.6[44]	109.4[45]	55.1[46]	92.7[13]

[a]Data correspond to single-point energy calculations at M06-2X/cc-pVTZ optimized geometries. Calculation of energy at the dissociation limit was done at an X−H distance of 5 Å and an X−X distance of 10 Å. [b]ZPVEs were added to the experimental dissociation energies. ZPVE values were taken from the Computational Chemistry Comparison and Benchmark DataBase[43] and correspond to CCSD(T)/cc-pVTZ values.

C−H bond in ethane. These trends are properly described by PNOF5, CASSCF, and CASPT2. However, PNOF5 predicts the O−H bond in H_2O_2 to be 3.5 kcal/mol stronger than the C−C bond in C_2H_6, while experimental evidence shows the opposite by 3.9 kcal/mol. CASSCF(2,2) behaves worse: O−H is 7.1 kcal/mol more stable than C−C, while this is corrected by CASPT2(2,2) which correctly predicts the C−C bond in ethane to be 5.5 kcal/mol stronger than the OH bond in hydrogen peroxide. Comparing X−X to X−H bond cleavage, one may observe that dynamical electron correlation plays a more important role in the former than in the latter. Thus, CASSCF(2,2) underestimates D_e by 22.4 and 35.7 kcal/mol for the C−C and O−O bonds, while this underestimation is much lower for the C−H and O−H bonds, namely, 20.4 and 11.4 kcal/mol, respectively. CASPT2 almost corrects this and leads to minimal errors, namely, 0.0, 1.4, 3.4, and 1.7 kcal/mol for C−C, O−O, C−H, and O−H bonds, respectively. PNOF5 results are between CASSCF and CASPT2 data. Differences from experimental values range from 6.1 kcal/mol for O−H to 22.5 kcal/mol for O−O bond. Clearly, it improves CASSCF results by roughly 10 kcal/mol but still lies approximately 10 kcal/mol from CASPT2 results. This again confirms the fact that PNOF5 is able to recover the strong correlation effects and a part of the dynamical electron correlation. The greater need to include dynamical electron correlation effects in the description of the bond strength on X−X bonds than in the X−H ones is the reason that accounts for the incorrect ordering between the C−C and O−H bonds in PNOF5.

In order to demonstrate the adequacy of the PNOF5 method to treat the strong correlation effects present in the formation of these radicals, we have investigated the change in highest occupied/lowest unoccupied molecular orbital (HOMO/LUMO) occupancies along the homolytic bond dissociation leading to radical formation and compared to the CASSCF ones. We selected as a test case the weak O−O bond in H_2O_2, and the results are depicted in Figure 3 . The agreement in HOMO/LUMO occupancies between PNOF5 and CASSCF methods is outstanding and indicates the correct description of the electronic structure in the whole potential energy surface (PES), including zones of the PES where strong electronic effects are dominant, that is, as we approach the dissociation limit forming two radicals. Note, however, that this agreement in occupancies does not necessarily imply that CASSCF and PNOF5 leads to the same electronic distribution. As we have

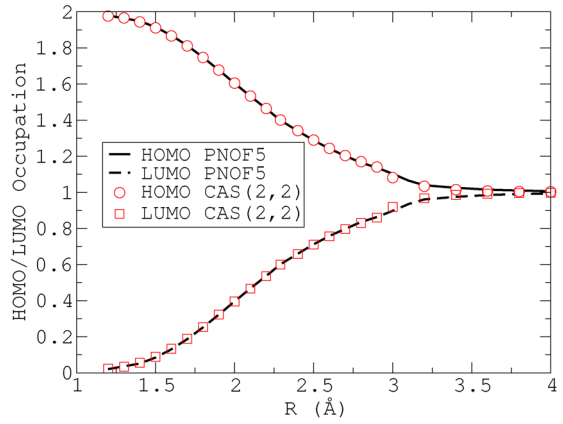

Figure 3. Agreement in HOMO/LUMO occupancies between PNOF5 and CASSCF methods for a selected case: O−O cleavage in hydrogen peroxide H_2O_2. The HOMO and LUMO orbitals correspond to a bonding σ_{O-O} and antibonding σ^*_{O-O} orbital, respectively.

seen previously,[33b] the electronic structure obtained with PNOF5 is more accurate than the one obtained with CASSCF wave functions, as indicated by the much better performance of PNOF5 in the description of dipole moments.

Hydrogen Abstraction Induced by Radicals. The results depicted in Tables 1 and 2 can be combined to yield thermodynamic data on the reaction energy of hydrogen abstraction reactions induced by radicals, as done previously by other authors.[47] In Table 3 we show these reaction energies, and in Figure 4, correlations among the theoretical and experimental data are depicted. As expected, very good results are obtained with CASPT2(2,2) with a MAE of only 1.3 kcal/mol and a linear correlation coefficient (r) with respect to experimental data of 0.9990. CASSCF(2,2) presents a MAE that is 1 order of magnitude larger, namely, 11.8 kcal/mol, and a poorer correlation coefficient, 0.9288. PNOF5 lies in between with a mean absolute error (MAE) of 7.4 kcal/mol and a correlation coefficient r of 0.9859.

A closer inspection of the values in Table 3 reveals that reactions in which hydroxyl radical is the hydrogen abstractor are favorable, with negative experimental values for the reaction energies between −33.3 and −10.1 kcal/mol. Similar values have been reported[14] for the exothermicities of hydroxyl attack on hydrides. However, those reactions in which the peroxyl radical is the hydrogen abstractor are unfavorable with high positive reaction energies (between 16.7 and 23.2 kcal/mol experimentally). PNOF5 is able to describe these trends, albeit with lower absolute values of the reaction energies. On the other hand, the $CH_4 + {}^{\bullet}NH_2 \rightarrow {}^{\bullet}CH_3 + NH_3$ reaction shows the lowest reaction energy in absolute value, −2.9 kcal/mol experimentally and −1.9 kcal/mol at CASPT2(2,2). An even lower value has been reported at the CCSD(T) level of theory,[14] that is, −0.9 kcal/mol. PNOF5 gives a positive value of the reaction energy, but of only 1.0 kcal/mol. The performance of PNOF5 is considerably superior to that of CASSCF(2,2), not only quantitatively but also qualitatively. Notice, for instance, that CASSCF(2,2) gives the wrong sign in the reaction energy for three out of the eight reactions considered. Nevertheless, PNOF5 also has limitations describing some of these reactions. For instance, hydrogen abstraction from methane and ethane shows the same reaction energy at PNOF5 level of theory, whereas both CASPT2 and

Table 3. Hydrogen Abstraction Reaction Energies Obtained by Combining the Data from Tables 1 and 2

	D_e (kcal/mol)			
	PNOF5	CASSCF(2.2)	CASPT2(2,2)	exptl
$CH_4 + {}^{\bullet}OH \rightarrow {}^{\bullet}CH_3 + H_2O$	−7.2	5.1	−13.2	−13.0
$CH_4 + {}^{\bullet}NH_2 \rightarrow {}^{\bullet}CH_3 + NH_3$	1.0	4.7	−1.9	−2.9
$NH_3 + {}^{\bullet}OH \rightarrow {}^{\bullet}NH_2 + H_2O$	−8.2	0.4	−11.3	−10.1
$C_2H_6 + {}^{\bullet}OH \rightarrow {}^{\bullet}C_2H_5 + H_2O$	−7.2	−3.7	−16.8	−16.6
$H_2O_2 + {}^{\bullet}OH \rightarrow HO_2{}^{\bullet} + H_2O$	−19.5	−11.6	−31.8	−33.3
$CH_4 + HO_2{}^{\bullet} \rightarrow {}^{\bullet}CH_3 + H_2O_2$	12.3	16.7	18.6	20.3
$NH_3 + HO_2{}^{\bullet} \rightarrow {}^{\bullet}NH_2 + H_2O_2$	11.3	12.0	20.5	23.2
$C_2H_6 + HO_2{}^{\bullet} \rightarrow {}^{\bullet}C_2H_5 + H_2O_2$	12.3	7.9	15.0	16.7
mean absolute error (MAE)	7.4	11.8	1.3	

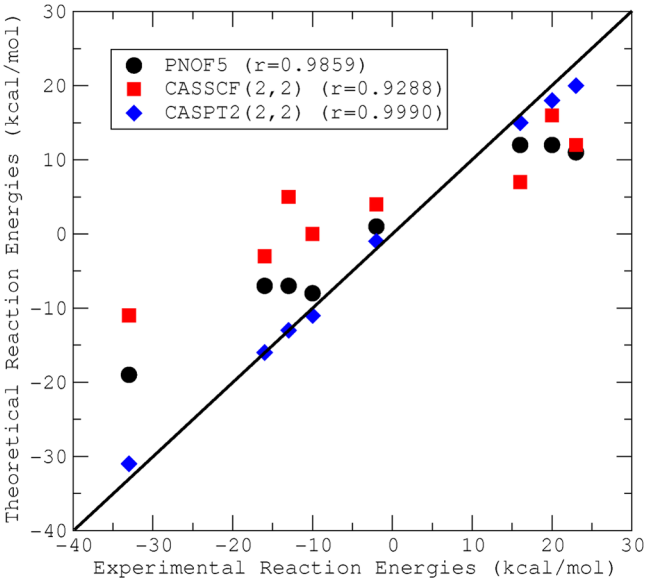

Figure 4. PNOF5, CASSCF(2,2), and CASPT2(2,2) hydrogen abstraction reaction energies versus experimental values. *r* stands for the linear correlation coefficients with respect to the experimental data.

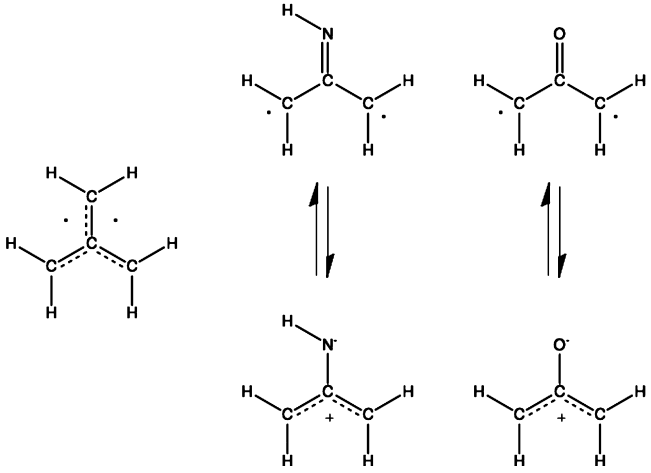

Figure 5. Trimethylenemethane (TMM), iminoallyl (IMA), and oxyallyl (OXA) molecules.

experimental values indicates an easier cleavage of the C−H bond in ethane by 3−4 kcal/mol.

Homolytic C−C Bond Cleavage in Cyclopropane and Derivatives. To further test the adequacy of PNOF5 to treat strong correlation effects in the cleavage of C−C bonds and formation of radicals, in this section we analyze C−C homolytic bond dissociation in a series of cyclopropanes: methylene cyclopropane (MCP), iminocyclopropane (IMCP), and cyclopropanone (OCP). Upon C−C cleavage we form a series of molecules that ranges from full to partial (di)radical character: trimethylenemethane (TMM), a molecule with two radical centers, iminoallyl (IMA), and oxyallyl (OXA) (see Figure 5), with the last two showing intermediate radical character. In a previous work,[32b] we analyzed this series of diradicals and diradicaloids at the PNOF4 level of theory. In Table 4, the natural orbital occupancies for the formal HOMO/LUMO orbitals can be found. In Table 5, we summarize the relevant energetic data, namely, the difference in energy between the cyclopropane derivative and its resultant products from the C−C cleavage.

The diradical character of the C−C cleavage products should decrease in the order TMM > IMA > OXA. In Table 4, we can investigate the degree of diradical character of these species. CASSCF methods give a very coherent picture, irrespective of the size of the window. For instance, at CASSCF(12,12), the largest diradical character corresponds to TMM (1.01/0.99), then to IMA (1.25/0.75), and finally to OXA (1.45/0.55). PNOF5 is able to reproduce these trends with occupancies of 1.00/1.00 for TMM, 1.26/0.74 for IMA, and 1.46/0.54 for OXA, a significant improvement over PNOF4.

On the other hand, the order in energy (see Table 5), TMM > IMA > OXA, reflects the order in diradical character of the product; however, these numbers are highly affected by the strong electron correlation upon C−C cleavage. Effectively, CASSCF methods lead to much lower relative energies than HF with values that vary depending on the size of the window: TMM (29.6−34.4) > IMA (23.3−34.0) > OXA (18.2−26.2). CASPT2 gives somewhat larger values with less variation with the size of the CAS window: TMM (43.5−43.3) > IMA (39.7−41.9) > OXA (32.6−36.0). PNOF5 shows the right order in energies with results that compare best with CASPT2: TMM (40.8) > IMA (37.2) > OXA (26.5). These values imply an improvement with respect to PNOF4, reducing the mean absolute error from 5.3 to 3.6 kcal/mol. In summary, the performance of PNOF5 to treat near-degeneracy effects and strong correlation effects in this type of C−C cleavage and radical formation is outstanding, and it implies a significant improvement with respect to PNOF4.

dx.doi.org/10.1021/ct300414t | J. Chem. Theory Comput. 2012, 8, 2646−2652

Table 4. Natural Orbital Occupancies for CASSCF, PNOF4, and PNOF5 Methods[a]

	TMM	MCP	IMA	IMCP	OXA	OCP
CASSCF(4,4)	1.02/0.99	1.97/0.02	1.21/0.80	1.97/0.03	1.40/0.60	1.97/0.03
CASSCF(12,12)	1.01/0.99	1.92/0.08	1.25/0.75	1.93/0.07	1.45/0.55	1.95/0.05
PNOF4	1.07/0.97	1.99/0.03	1.36/0.71	1.98/0.04	1.57/0.50	1.98/0.05
PNOF5	1.00/1.00	1.92/0.08	1.26/0.74	1.92/0.08	1.46/0.54	1.99/0.01

[a]CASSCF, CASPT2, and PNOF4 data were taken from ref 32b. Geometries were optimized at the CASSCF(4,4)/cc-pVDZ level of theory.

Table 5. Thermodynamics of C−C Cleavage

	relative energy[a] (kcal/mol)		
	MCP → TMM	IMCP → IMA	OCP → OXA
HF	94.6	74.7	55.7
CASSCF(4,4)	29.6	23.3	18.2
CASPT2(4,4)	43.5	41.9	36.0
CASSCF(12,12)	34.4	34.0	26.2
CASPT2(12,12)	43.3	39.7	32.6
PNOF4	49.5	45.0	36.6
PNOF5	40.8	37.2	26.5

[a]Relative energies for TMM, IMA, and OXA diradicals and diradicaloids with respect to their corresponding cyclic MCP, IMCP, and OCP cyclopropane derivatives are given. CASSCF, CASPT2, and PNOF4 data were taken from ref 32b. Geometries were optimized at the CASSCF(4,4)/cc-pVDZ level of theory.

CONCLUSIONS

In summary, we have demonstrated that natural orbital functional theory (NOFT) in its PNOF5 implementation can describe in a balanced way chemical bonding situations that evolve gradually from nondegenerate to degenerate states, giving an outstanding description of the strong correlation effects found in the formation of radicals from homolysis of covalent bonds. We have shown that PNOF5 is able to reproduce the dissociation curves of a series of X−H bonds in selected hydrides. In addition, it gives a good description of the cleavage of X−H bonds in comparison with X−X cleavage in X_2H_n-type molecules. The bond dissociation energies can then be combined to yield reaction energies for hydrogen abstraction reactions induced by radicals. We have found that the PNOF5 description of these reaction energies is satisfactory and superior to the CASSCF method, with a window size sufficient to consider near-degeneracy effects. Finally, in the case of cyclopropanone and its derivatives, we have seen that PNOF5 yields the right description of full and partial diradical character upon C−C bond cleavage, being superior to previous versions of the PNOF functional. Differences between experimental and CASPT2 dissociation energies with PNOF5 can be ascribed to a partial lack of dynamical electron correlation, whereas the description of the nondynamical part, the cumbersome problem in electronic structure theory, seems to be accounted for well by PNOF5, as revealed by the agreement in natural orbital occupancies of CASSCF methods. Therefore, PNOF5 appears as an alternative method to treat problems such as hydrogen abstraction and homolytic bond cleavage for which wave function methods are prohibitive to apply and DFT methods dramatically fail at strong correlation effects. In this sense, one should remark the more favorable scaling of PNOF5 (on the order of mN^4, with N = number of basis functions and m = number of iterations) over CASSCF (nN^6, with n = window size). Future research will consider the application of PNOF5 to describe hydrogen abstraction in longer aliphatic chains and in (poly)peptides. Studies along these lines are under way.

ASSOCIATED CONTENT

Supporting Information

Two tables listing X−H bond dissociation energies for methane, ammonia, water, ethane, and hydrogen peroxide along with X−X dissociation energies for ethane and hydrogen peroxide, calculated at CASSCF and CASPT2 levels of theory with several basis sets and different window sizes. This material is available free of charge via the Internet at http://pubs.acs.org/

AUTHOR INFORMATION

Corresponding Author

*E-mail xabier.lopez@ehu.es.

Notes

The authors declare no competing financial interest.

ACKNOWLEDGMENTS

Financial support comes from Eusko Jaurlaritza (GIC 07/85 IT-330-07) and the Spanish Office for Scientific Research (CTQ2011-27374). The SGI/IZO−SGIker UPV/EHU is gratefully acknowledged for generous allocation of computational resources. J.M.M. thanks the Spanish Ministry of Science and Innovation for a Ramon y Cajal fellowship (RYC 2008-03216). In addition, funding from the SAIOTEK program (S-PC11UN003, Basque Government) is also acknowledged. E.M. acknowledges financial support of the EU under a Marie Curie Career Integration grant (PCI09-GA-2011-294240) and the Beatriu de Pinós program from AGAUR for the postdoctoral grant (BP_B_00236).

REFERENCES

(1) Valko, M.; Rhodes, C. J.; Moncol, J.; Izakovic, M.; Mazur, M. *Chem.-Biol. Interact.* **2006**, *160*, 1−40.
(2) Breher, F. *Coord. Chem. Rev.* **2007**, *251*, 1007−1043.
(3) Dietl, N.; Schlangen, M.; Schwarz, H. *Angew. Chem., Int. Ed.* **2012**, *51*, 5544−5555.
(4) Stadtman, E. R.; Levine, R. L. *Amino Acids* **2003**, *25*, 207−18.
(5) Lushchak, V. I. *Biochemistry (Moscow)* **2007**, *72*, 809−827.
(6) Davies, K. J.; Lin, S. W; Pacifici, R. E. *J. Biol. Chem.* **1987**, *262*, 9914−9920.
(7) Valko, M.; Leibfritz, D.; Moncol, J.; Cronin, M. T. D.; Mazur, M.; Telser, J. *Int. J. Biochem. Cell Biol.* **2007**, *39*, 44−84.
(8) Halliwell, J. G. B. *Free Radicals in Biology and Medicine*; Oxford University Press: Oxford, U.K., 1999.
(9) Korchowiec, J. *J. Phys. Org. Chem.* **2002**, *15*, 524−528.
(10) Luga, C.; Ignacio Sainz-Díaz, C.; Vivier-Bunge, A. *Geochim. Cosmochim. Acta* **2010**, *74*, 3587−3597.
(11) Prousek, J. *Pure Appl. Chem.* **2007**, *79*, 2325−2338.
(12) Balasubramanian, B.; Pogozelski, W. K.; Tullius, T. D. *Proc. Natl. Acad. Sci. U.S.A.* **1998**, *95*, 9738−43.
(13) Ramond, T.; Blanksby, S.; Kato, S. *J. Phys. Chem. A* **2002**, *106*, 9641−9647.
(14) Basch, H.; Hoz, S. *J. Phys. Chem. A* **1997**, *101*, 4416−4431.
(15) Temelso, B.; Sherrill, C. D.; Merkle, R. C.; Freitas, R. a. *J. Phys. Chem. A* **2006**, *110*, 11160−11173.

(16) Vandeputte, A. G.; Sabbe, M. K.; Reyniers, M. F.; Van Speybroeck, V.; Waroquier, M.; Marin, G. B. *J. Phys. Chem. A* **2007**, *111*, 11771−11786.
(17) Cramer, C. J.; Truhlar, D. G. *Phys. Chem. Chem. Phys.* **2009**, *11*, 10757−10816.
(18) (a) Gilbert, T. L. *Phys. Rev. B* **1975**, *12*, 2111. (b) Levy, M. *Proc. Natl. Acad. Sci. U.S.A.* **1979**, *76*, 6062. (c) Valone, S. M. *J. Chem. Phys.* **1980**, *73*, 1344.
(19) Gritsenko, O. V.; Pernal, K.; Baerends, E. J. *J. Chem. Phys.* **2005**, *122*, No. 204102.
(20) Frank, R. L.; Lieb, E. H.; Seiringer, R.; Siedentop, H. *Phys. Rev. A* **2007**, *76*, No. 052517.
(21) Rohr, D. R.; Pernal, K.; Gritsenko, O. V.; Baerends, E. J. *J. Chem. Phys.* **2008**, *129*, No. 164105.
(22) Marques, M. A. L.; Lathiotakis, N. N. *Phys. Rev. A* **2008**, *77*, No. 032509.
(23) Sharma, S.; Dewhurst, J. K.; Lathiotakis, N. N.; Gross, E. K. U. *Phys. Rev. B* **2008**, *78*, No. 201103.
(24) Lathiotakis, N. N.; Sharma, S.; Dewhurst, J. K.; Eich, F. G.; Marquers, M. A. L.; Gross, E. K. U. *Phys. Rev. A* **2009**, *79*, No. 040501.
(25) Lathiotakis, N. N.; Helbig, N.; Zacarias, A.; Gross, E. K. U. *J. Chem. Phys.* **2009**, *130*, No. 064109.
(26) Tsuchimochi, T.; Scuseria, G. E. *J. Chem. Phys.* **2009**, *131*, No. 121102.
(27) Piris, M. *Adv. Chem. Phys.* **2007**, *134*, 387.
(28) Piris, M. *Int. J. Quantum Chem.* **2012**, DOI: 10.1002/qua.24020.
(29) (a) Leiva, P.; Piris, M. *J. Chem. Phys.* **2005**, *123*, No. 214102;(b) *J. Theor. Comput. Chem.* **2005**, *4*, 1165;(c) *J. Mol. Struct.: THEOCHEM* **2006**, *770*, 45;(d) *Int. J. Quantum Chem.* **2007**, *107*, 1. (e) Piris, M.; Matxain, J. M.; Lopez, X.; Ugalde, J. M. *J. Chem. Phys.* **2009**, *131*, No. 021102.
(30) (a) Piris, M.; Lopez, X.; Ugalde, J. M. *J. Chem. Phys.* **2007**, *126*, No. 214103;(b) *Int. J. Quantum Chem.* **2008**, *108*, 1660;(c) *J. Chem. Phys.* **2008**, *128*, No. 134102. (d) Piris, M.; Matxain, J. M.; Ugalde, J. M. *J. Chem. Phys.* **2008**, *129*, No. 014108.
(31) (a) Piris, M.; Matxain, J. M.; Lopez, X.; Ugalde, J. M. *J. Chem. Phys.* **2010**, *132*, No. 031103. (b) Lopez, X.; Piris, M.; Matxain, J. M.; Ugalde, J. M. *Phys. Chem. Chem. Phys.* **2010**, *12*, 12931. (c) Matxain, J. M.; Piris, M.; Lopez, X.; Ugalde, J. M. *Chem. Phys. Lett.* **2010**, *499*, 164.
(32) (a) Piris, M.; Matxain, J. M.; Lopez, X.; Ugalde, J. M. *J. Chem. Phys.* **2010**, *133*, No. 111101. (b) Lopez, X.; Ruipérez, F.; Piris, M.; Matxain, J. M.; Ugalde, J. M. *ChemPhysChem* **2011**, *12*, 1061. (c) Lopez, X.; Piris, M.; Matxain, J. M.; Ruipérez, F.; Ugalde, J. M. *ChemPhysChem* **2011**, *12*, 1673.
(33) (a) Piris, M.; Lopez, X.; Ruipérez, F.; Matxain, J. M.; Ugalde, J. M. *J. Chem. Phys.* **2011**, *134*, No. 164102. (b) Matxain, J. M.; Piris, M.; Ruipérez, F.; Lopez, X.; Ugalde, J. M. *Phys. Chem. Chem. Phys.* **2011**, *13*, 20129. (c) Matxain, J. M.; Piris, M.; Mercero, J. M.; Lopez, X.; Ugalde, J. M. *Chem. Phys. Lett.* **2012**, DOI: 10.11016/j.cplett.2012.02.041.
(34) Van Aggelen, H.; Bultinck, P.; Verstichel, B.; Van Neck, D.; Ayers, P. W. *Phys. Chem. Chem. Phys.* **2009**, *11*, 5558.
(35) Van Aggelen, H.; Verstichel, B.; Bultinck, P.; Van Neck, D.; Ayers, P. W.; Cooper, D. L. *J. Chem. Phys.* **2010**, *132*, No. 114112.
(36) Zhao, Y.; Truhlar, D. G. *Theor. Chem. Acc.* **2008**, *120*, 215−241.
(37) Dunning, T. H. *J. Chem. Phys.* **1989**, *90*, 1007.
(38) Frisch, M. J.; Trucks, G. W.; Schlegel, H. B.; Scuseria, G. E.; Robb, M. A.; Cheeseman, J. R.; Scalmani, G.; Barone, V.; Mennucci, B.; Petersson, G. A.; Nakatsuji, H.; Caricato, M.; Li, X.; Hratchian, H. P.; Izmaylov, A. F.; Bloino, J.; Zheng, G.; Sonnenberg, J. L.; Hada, M.; Ehara, M.; Toyota, K.; Fukuda, R.; Hasegawa, J.; Ishida, M.; Nakajima, T.; Honda, Y.; Kitao, O.; Nakai, H.; Vreven, T.; Montgomery, J. A., Jr.; Peralta, J. E.; Ogliaro, F.; Bearpark, M.; Heyd, J. J.; Brothers, E.; Kudin, K. N.; Staroverov, V. N.; Kobayashi, R.; Normand, J.; Raghavachari, K.; Rendell, A.; Burant, J. C.; Iyengar, S. S.; Tomasi, J.; Cossi, M.; Rega, N.; Millam, J. M.; Klene, M.; Knox, J. E.; Cross, J. B.; Bakken, V.; Adamo, C.; Jaramillo, J.; Gomperts, R.; Stratmann, R. E.; Yazyev, O.; Austin, A. J.; Cammi, R.; Pomelli, C.; Ochterski, J. W.; Martin, R. L.; Morokuma, K.; Zakrzewski, V. G.; Voth, G. A.; Salvador P.; Dannenberg, J. J.; Dapprich, S.; Daniels, A. D.; Farkas, O.; Foresman, J. B.; Ortiz, J. V.; Cioslowski, J.; Fox, D. J. *Gaussian 09, Revision A.1*; Gaussian Inc., Wallingford, CT, 2009.
(39) Aquilante, F.; De Vico, L.; Ferré, N.; Ghigo, G.; Malmqvist, P.-Å.; Neogrády, P.; Pedersen, T. B.; Pitoňák, M.; Reiher, M.; Roos, B. O.; Serrano-Andrés, L.; Urban, M.; Veryazov, V.; Lindh, R. *J. Comput. Chem.* **2010**, *31*, 224.
(40) Piris, M. *PNOFID: Iterative diagonalization for orbital optimization using the PNOF*; downloadable at http://www.ehu.es/mario.piris/#Software.
(41) Piris, M.; Ugalde, J. M. *J. Comput. Chem.* **2009**, *30*, 2078−2086.
(42) Ervin, K.; DeTuri, V. *J. Phys. Chem. A* **2002**, *106*, 9947−9956.
(43) NIST Computational Chemistry Comparison and Benchmark Database; NIST Standard Reference Database Number 101, Release 15b, August 2011; Editor: Johnson, R. D., III; http://cccbdb.nist.gov/ (accessed Feb 15, 2012).
(44) Pesa, M.; Pilling, M. J.; Robertson, S. H.; Wardlaw, D. M. *J. Phys. Chem. A* **1998**, *102*, 8526−8536.
(45) Bauschlicher, C. W.; Partridge, H. *Chem. Phys. Lett.* **1995**, *2614*, 246−251.
(46) Bach, R.; Ayala, P. *J. Am. Chem. Soc.* **1996**, *2*, 12758−12765.
(47) Menon, A. S.; Wood, G. P. F.; Moran, D.; Radom, L. *J. Phys. Chem. A* **2007**, *111*, 13638.